Novel microfluidic graphene oxide–protein amperometric biosensor for detecting sulfur compounds

Amirhossein Ghaemi[1]
Kaveh Abdi[2]
Shohreh Javadi[3]
Masoud Zare Shehneh[4]
Fatemeh Yazdian[1*]
Meisam Omidi[5,6*]
Hamid Rashedi[7]
Bibi Fatemeh Haghiralsadat[8]
Omid Asayeshnaeini[1]

[1] *Department of Life Science Engineering, Faculty of New Science and Technology, University of Tehran, Tehran, Iran*

[2] *Chemical and Petroleum Engineering Department, Sharif University of Technology, Tehran, Iran*

[3] *Chemical Engineering Department, Ferdowsi University of Mashhad, Mashhad, Iran*

[4] *Genetic department, Shahid Sadoughi University of Medical Sciences, Yazd, Iran*

[5] *Marquette University School of Dentistry, Milwaukee, WI, USA*

[6] *Protein Research Centre, Shahid Beheshti University, GC, Velenjak, Tehran, Iran*

[7] *Department of Chemical Engineering, Faculty of Engineering, University of Tehran, Tehran, Iran*

[8] *Department of Advanced Medical Sciences and Technologies, School of Paramedicine, Shahid Sadoughi University of Medical Sciences, Yazd, Iran*

Abstract

Sulfur compounds are essential for many industries and organisms; however, they cause serious respiratory problems in human beings. Therefore, determination of sulfur concentration is of paramount importance. The research approach in the field of detecting contaminants has led to smaller systems that provide faster and more effective ways for diagnosis purposes. In this study, a novel portable amperometric graphene oxide–protein biosensor platform is investigated. The main characteristic of this structure is the implementation of a microfluidic configuration. With albumin metalloprotein as the biorecognition element, graphene oxide was synthesized and characterized by transmission electron microscopy and Fourier-transform infrared spectroscopy (FTIR). Albumin protein was stabilized on the surface of graphene oxide by the application of the N-(3-dimethylamionpropyl)-N-ethylcarbodiimide hydrochloride/N-hydroxysuccinimide method. The stabilization was confirmed by FTIR and electrochemistry analyses. The calibration curve of sulfur concentration was determined. When the graphene oxide–protein complex was stabilized by nephion on the surface of the microfluidic system, the response time reduced to 50 Sec, which is a relatively faster response among the similar studies and validated the significant effect of the microfluidic system. The nanosystem had an optimized pH of 7.4 and exhibited high sensitivity in determining sulfide. The results confirm that the portable graphene oxide–protein nanosystem has a fast and accurate response in detecting sulfide. Volume 66, Number 3, Pages 353–360, 2019

Keywords: *albumin metalloprotein, biosensor, graphene oxide, microfluidic, sulfur detection*

Abbreviations: *CaS, calcium sulfide; CCD, central composite design; C_2H_6O, ethanol; EDC, N-(3-dimethylamionpropyl)-N-ethylcarbodiimide hydrochloride; FTIR, Fourier-transform infrared spectroscopy; GO, graphene oxide; HCl, hydrochloric acid; H_2SO_4, sulfuric acid; NHS, N-hydroxysuccinimide; $NaNO_3$, sodium nitrate; NaOH, sodium hydroxide; PBS, phosphate-buffered saline; TEM, transmission electron microscope.*

**Address for correspondence: Fatemeh Yazdian, PhD, Department of Life Science Engineering, Faculty of New Science and Technology, University of Tehran, Tehran, Iran. email: Yazdian@ut.ac.ir; or Meisam Omidi, Protein Research Centre, Shahid Beheshti University, GC, Velenjak, Tehran, Iran; Marquette University School of Dentistry, Milwaukee, WI, USA. Tel: +982186093259; Fax: +982188497324; e-mail: m_omidi@sbu.ac.ir.*

Received 27 October 2018; accepted 10 December 2018

DOI: 10.1002/bab.1731

Published online 8 February 2019 in Wiley Online Library (wileyonlinelibrary.com)

1. Introduction

Sulfur compounds are important for the metabolism of organisms, the environment, and many other applications such as paper, oil, petrochemical, and textile industries [1–3]. Nonetheless, sulfide is considered toxic to the human body; it stimulates the mucous membrane and even leads to anesthesia and respiratory paralysis [4]. It has high reactivity as well, as a result of which the risk of exposure, which might cause health-endangering effects, becomes highly important. Therefore, the local anion concentration prompts significant safety and concern constraints for those working in environments containing sulfide species [5]. Moreover, determination of sulfide species concentration is a key for several researches ranging from groundwater monitoring to biogeochemical process investigation in hydrothermal vent fluids and aquatic sediment porewaters [4]. Consequently, having in mind the significance of sulfide species concentration and the effects of exposure to these species, developing a technique that can measure the concentration of sulfide species is of great importance.

A broad spectrum of methods, including iodic methods [6, 7], polarography [8], spectrophotometry [4, 9], chromatography [10], potentiometry [11], amperometry [12–15], voltammetry [16, 17], and surface plasmon resonance [18, 19], has been used for detection of sulfide species. Among these methods, biosensors have received extensive attention [20] because of their significant advantages including high selectivity, fast response [15, 21], and real-time analysis [22]. Different types of biosensors are widely studied for detecting pathogenic organisms, carcinogenic, mutagenic, and toxic chemicals or in order to inform about the biological response [23].

Among the various biosensor methods, the ones that are less time consuming [22], portable, and efficient in on-site detection of multi-pollutants [24] take priority over the other ones. As a result, electrochemical techniques, which not only have the advantage of quick response but are also simple to use and low cost, have been applied for sulfide detection [25–27].

Different bioelements have been used in order to detect sulfide species by using electrochemical techniques. For instance, Albery et al. [28] used the cytochrome oxidase respiratory enzyme in order to detect toxic gases, such as hydrogen sulfide (H_2S) and hydrogen cyanide, showing inhibitory properties at low concentrations. Another inhibitory enzyme used in the detection of sulfide species is ascorbic oxidase, which was used by Poor et al. [29] to detect H_2S. In another work, sulfide-oxidizing bacteria was used by Janfada et al. [30] in an H_2S detection system. Detection of the sulfide species by using biosensors has been focused more on enzyme-based biosensors [13, 22, 31]. Therefore, using other bioelements such as proteins can be considered promising.

Microfluidic lab-on-a-chip devices have drawn significant attention in recent years because of their unique characteristics including short time assay [32, 33], requiring low reagent volume [32, 33], having the ability to integrate multiple processes into one platform [32, 34], low-cost production [35], and simple process control [35].

In this study, a microfluidic graphene-based amperometric biosensor platform to detect sulfide is investigated. Graphene oxide was applied to enhance the reaction surface and served as a suitable substrate for the biorecognition element. The biorecognition element is metalloproteinase albumin that sulfide species oxidize, which leads to the generation of a signal and consequently, obtaining a calibration curve. It is also shown that the relationship between the signal and the sulfide concentration is linear in the range of 0.5–5 μM with a detection limit of 0.5 μM. Furthermore, the microfluidic assay response time is compared with the glassy carbon, indicating that the response time of the microfluidic system is less than one-third of the glassy carbon system, which proves the effective role of applying microfluidic system.

2. Materials and Methods

2.1. Materials and chemicals

Sodium hydroxide (NaOH), hydrochloric acid (HCl), sulfuric acid (H_2SO_4), sodium nitrate ($NaNO_3$), and ethanol (C_2H_6O) were purchased from Merck, whereas N-(3-dimethylamionpropyl)-N-ethylcarbodiimide hydrochloride (EDC) and N-hydroxysuccinimide (NHS) were purchased from Sigma. Also, graphite powder and calcium sulfide (CaS) were used in the experiments. Albumin protein as the bioreceptor was provided from Sigma (A9647). All the chemicals were utilized without further purifications.

2.2. Preparation of graphene oxide solution

First, graphene oxide was prepared by the modified Hummer's method [36]. The result was a brilliant yellow product that was purified by HCl and deionized water. In order to prepare 1 mg/mL graphene oxide solution, deionized water (20 mL) was added to graphene oxide sheets (20 mg). The solution was put into an ultrasonic bath, where it was first sonicated for 30 Min and then ultra-sonicated for 5 Min, which led to the formation of a light brown homogeneous solution.

2.3. Characterization of graphene oxide

To study the surface structure of the produced nanostructures, transmission electron microscope (TEM) images were analyzed. The chemical composition of the nanostructures was studied by Fourier-transform infrared spectroscopy (FTIR).

2.4. Stabilization of albumin protein on graphene oxide

In the current work, the protocol presented in *Bioconjugate Techniques* by Hermanson [37] used to stabilize albumin protein on the surface of graphene oxide nanohybrid was applied. In brief, the two-step conjugation was as follows: after synthesis of the nanohybrid sample under optimized conditions by centrifugation, the upper part was replaced with 0.1 M phosphate-buffered saline (PBS) and the sample was placed in the ultrasonic bath and sonicated for 25 Min. Then, it was

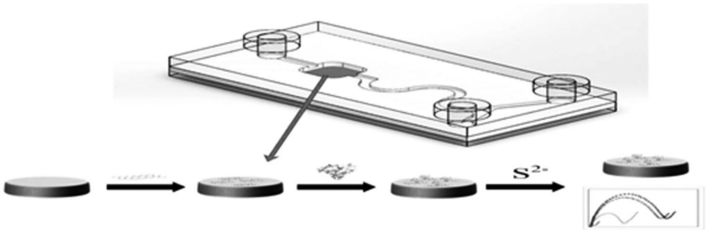

FIG. 1 *Structure and channels of the designed microfluidic system and steps of embedding electrodes in channels.*

ultra-sonicated for 5 Min to form a homogenous mixture that was ready for albumin protein stabilization. The next step involved the functionalization of graphene oxide. For this purpose, EDC/sulfo-NHS was used, and the same amount of conjugators was added to the mixture. The mixture was stirred at 275 rpm at room temperature for 15 Min. Bovine serum albumin solution was added to the mixture where it reacted for 2 H. To prepare the albumin solution, the concentration of albumin was considered equal to that of graphene (0.07 mg/mL). The solution was centrifuged (1521 $\times g$, 10 Min) and the upper part was replaced by PBS to remove the extra conjugators.

2.5. Characterization of nanohybrid

The stabilization of protein on graphene oxide was studied by FTIR, and amperometry tests were done by a Potentiostat device (vertex one, EVUM). The protein–graphene oxide system was placed as work and reference electrodes embedded in the potentiostat cell.

2.6. Microfluidic system

The microfluidic system was prepared by soft lithography in The Protein Research Center of Shahid Beheshti University. Figure 1 shows its structure and channels.

At first, nephion was used for locating the graphene oxide–protein nanosystem. 1% graphene oxide–protein was put into 0.1% nephion solution on the surface of the microfluidic system and placed in a spin coater (2500 rpm) to achieve the desired thickness, uniformity, and distribution. Next, it was allowed to dry for 30 Min. A copper wire (100 μm) and a silver wire (100 μm) were connected to the system such that the end of the silver wire (considered as the work electrode) was connected to the convectional three-electrode potentiostat system. After that, different concentrations of sulfide were injected into the system by a syringe pump (100 μL/Min). Eventually, the characteristics of the nanosystem were determined according to the changes in amperometry flow.

2.7. Response time

To measure the response time, a cell consist of both the working electrode and reference electrode in the presence of sulfide at the optimized pH was prepared. The amperometry variations through time were recorded. Previous researchers defined the response time of a nanosystem based on amperometry variations as the time when the curve reaches a stable steady-state after some pulsations [38].

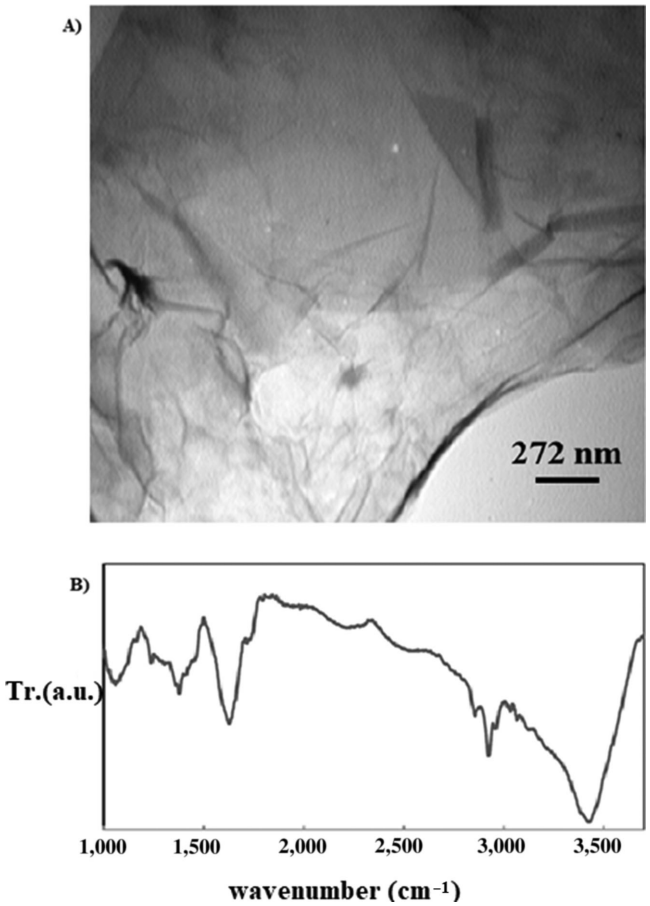

FIG. 2 *(A) TEM images of graphene oxide. (B) FTIR spectrum of graphene oxide.*

2.8. Determination of the detection limit

Based on previous studies, the detection limit was determined by the 3λ method in this work. Λ is the error and noise of the device, which is shown as error bars in the calibration curve. Based on this value, 3λ/slop of the calibration curve is the detection limit of the device [39].

3. Results and Discussion

3.1. Characterization of graphene oxide

Graphene oxide was characterized by TEM and FTIR. Figure 2A shows the TEM image of the synthesized graphene oxide. It exhibits a single layer of graphene proving the high quality of synthesized graphene oxide.

FTIR spectra were used to study graphene oxide bonding. Figure 2B exhibits the FTIR spectra corresponding to the synthesized graphene oxide. It can be seen that the peaks are at 1,050 cm^{-1} (C—O stretching), 1,200 cm^{-1} (C—O—C stretching), 1,600 cm^{-1} (COOH stretching), and 1,700 cm^{-1}

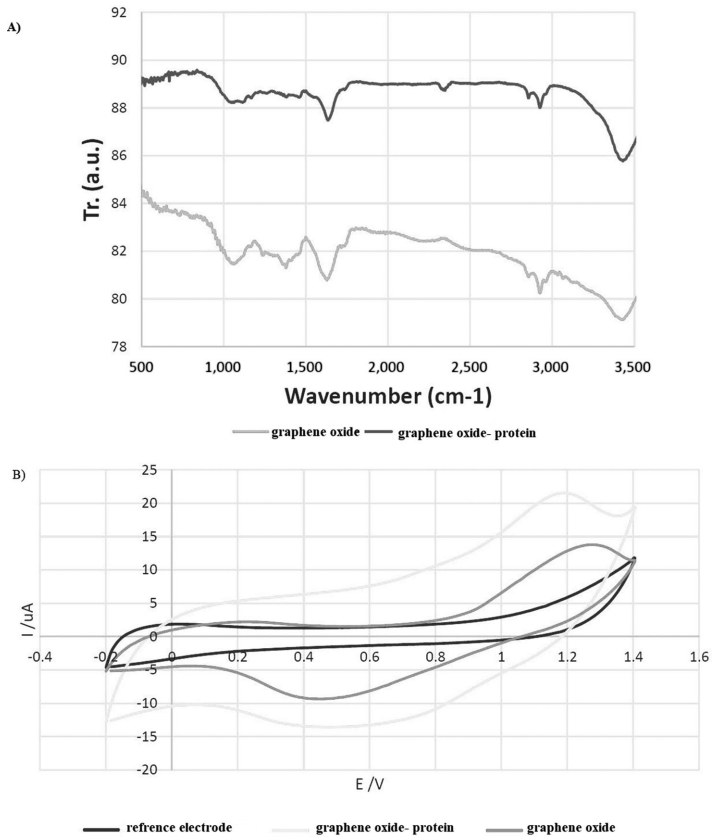

FIG. 3 *(A) FTIR curve of graphene oxide and graphene oxide–albumin protein. (B) Voltagram curve of carbon, electrode, graphene oxide, and graphene oxide–protein.*

(C═O stretching). There is also a broad band having peaks at 3,000–3,700 cm^{-1} representing hydroxyl groups (C─OH stretching). The existence of oxygenated functional groups implies that graphene oxidized perfectly. These results are consistent with the FTIR results of previous studies on graphene oxide sheets, which confirms our findings. For example, Rana et al. [40] reported 1,726 cm^{-1} for the C═O stretching and 1,223 cm^{-1} for the C─O─C stretching in their work.

3.2. Characterization of nanohybrid

Figure 3A shows the stabilization of protein on graphene oxide. As can be seen, the absorption intensity is higher for the graphene oxide–albumin protein than graphene oxide alone, and it can be concluded that stabilization of the protein influenced the amount and range of the peaks. Another test for characterizing nanohybrids is the electrochemistry method. Figure 3B exhibits the variations of electrodes' voltammogram (glassy carbon, graphene oxide, and graphene oxide–protein). The area under the curve is larger for graphene oxide than the other electrodes, which indicates the unique ability of graphene oxide for electron exchange.

The role of sulfide in the current configuration is that in its presence in the dual-core protein center, the protein reduces by

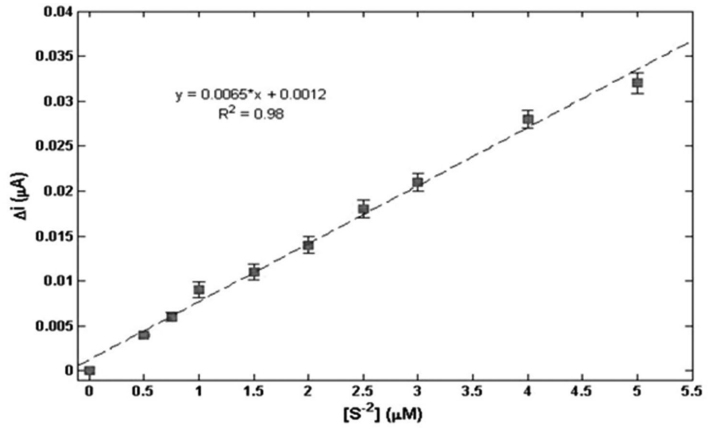

FIG. 4 *Calibration curve of stabilized protein at 0–5.5 μM sulfide concentration.*

sulfide compound and supplies its electron from sulfide instead of the electrode. As a result, the reduction peaks decrease slowly. In the cyclic voltammetry method, peaks of oxidation and reduction are interdependent. That means reduction and oxidation peaks reduce by the same amount. Thus, in consecutive cycles, the oxidation peaks reduce precisely as do the reduction peaks.

3.3. Calibration curve of sulfur concentration and detection limit

The relationship between the sulfide ion concentration and the amperometric current change is shown in Fig. 4. As demonstrated in this figure, by increasing the sulfide concentration, the current pulse also increases, and there is a linear relationship in the range of 0.5–5 μM with a correlation coefficient of 0.98 between sulfide concentrations and current changes. The detection limit was found to be 0.5 μM by the 3λ method from the calibration curve. Poor et al. [29] studied H_2S detection and reported a linear relationship in the range of 1–15 mg/L between oxygen and H_2S concentration and a detection limit of 0.5 mg/L. Mirzaei et al. [41] reported a detection limit of 0.5 mg/L in the range of 1–20 mg/L for H_2S detection. Salamanca-Neto et al. [42] designed a voltammetry biosensor and stated 2.59 μM as their detection limit in the sulfur concentration range of 9.94–271 μM. Other reported data related to detection of sulfur compounds are presented in Table 1.

3.4. Effect of pH on the nanosystem

To identify the effect of pH on the current changes for different sulfide concentrations, the experiments were conducted at three different pH values of 6.4, 7.4, and 8.4. As can be seen in Fig. 5, by increasing the concentration, the highest current changes can be observed for pH = 7.4 in comparison with other pHs. Li et al. [43] related the same pH for H_2S detection. Poor et al. [29] reported pH = 7 as the optimum pH for H_2S detection. Ghadiri et al. [44], Savizi et al. [22], and Liu et al. [25] observed maximum inhibition of sulfide at pH = 6.5. Li

TABLE 1 *Comparison of other studies on detection of sulfur compounds*

Author	*Recognized compound/element*	*Bio-recognition element*	*Optimized pH*	*Range*	*Detection limit*	*Response time (Sec)*
Liu et al. [25]	Sulfide	Horseradish peroxidase	6.5	0.1–38.5 μM	0.05 μM	65
Savizi et al. [22]	Sulfide	Copinus cinerus peroxidase	6.5	1.09–16.3 μM	0.3 μM	43
Ghadiri et al. [44]	Sulfide	Fungal peroxidase	6.5	0.6–7 μM	0.4 μM	43
Poor et al. [29]	Hydrogen sulfide	Ascorbate oxidase	7	1–15 mg/L	0.5 mg/L	55
Mirzaei et al. [41]	Hydrogen sulfide	Thiobacillus thioparus	7	1–20 mg/L	0.5 mg/L	80
Vosoughi et al. [49]	Hydrogen sulfide	Thiobacillus thioparus	7	0.5–20 ppm	0.5 ppm	72
Liu et al. [3]	sulfide	Recombinant Escherichia coli BL21	-	50–500 μM	2.55 μM	-
Li et al. [50]	Hydrogen sulfide	UiO-66-CH=CH_2	7.4	10–600 μM	6.46 μM	10
Neto et al. [42]	sulfide	Triphenylphosphine	-	9.94–271 μM	2.59 μM	-
Li et al. [45]	Sulfur dioxide	–	Not sensitive to pH changes	0–18 μM	0.504 μM	300
In this study	Sulfide	Metalloprotein albumin	7.4	0.5–5 μM	0.5 μM	50

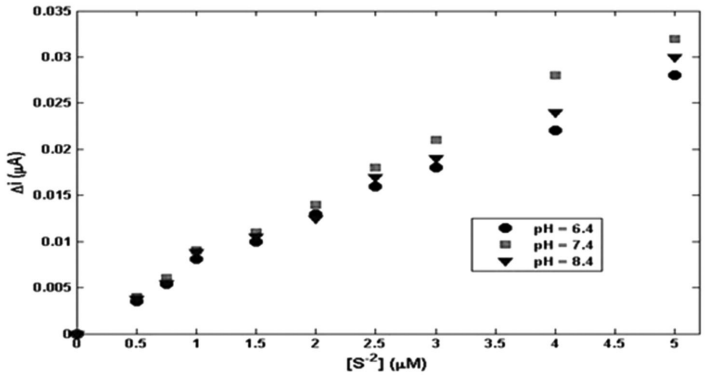

FIG. 5 *Current difference for stabilized protein in the presence of 0–5 μM sulfide at different pH values.*

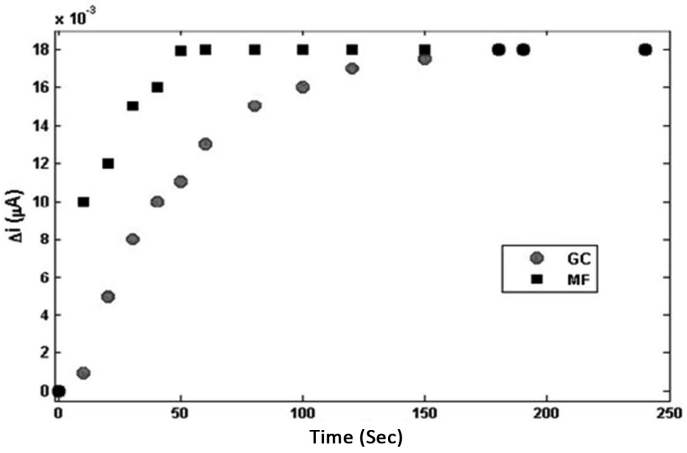

FIG. 6 *The first recognizable response in Voltagrams of stabilized protein after sulfide injection.*

et al. [45] observed insensitivity of their designed sensor to pH changes. The other pH optimization results are summarized in Table 1.

3.5. Response time measurement

In order to assess the performance of the microfluidic system, a comparison was made between the microfluidic system containing the protein–graphene oxide working electrode and the glassy carbon containing protein–graphene oxide working electrode at the optimal pH obtained in the last section. The protein reacts with sulfide in both cells (consisting of work and the reference electrode and injected sulfide) and the amperometry variations through time were recorded and used to prepare Fig. 6. As can be seen, the microfluidic system reaches stable steady-state condition much sooner than the glassy carbon system, which shows the lower response time of the microfluidic biosensor (50 Sec) than the glassy carbon (175 Sec). The prime reason for this remarkable decrease in the response time is applying the microfluidic system. To explain the exact reason, during the transmission of fluid from microtubes, Reynolds number decreased and the reaction surface increased, which both had improvement

effect on accelerating the reaction and also response time of the microfluidic biosensor. Although the existence of graphene oxide with high surface area provided more surface for the reaction between sulfide and albumin protein and affected the response time.

As the amount of pollutants in the environment are rising, the importance of finding a fast and sensitive detection method becomes more [46]. The results show the lower response time compared with Liu et al. [25], Poor et al. [29], Janfada et al. [30], Wen et al. [47], Mirzaei et al. [41], and Omidi et al. [19]. It should be noted that Ghadiri et al. [44], Savizi et al. [22], and Li et al. [43] reported a lower response time (43 Sec) in their works.

The results of other studies on the detection of sulfur compounds are summarized in Table 1. It shows obviously that the microfluidic graphene oxide–protein biosensor improved the sulfur detection rate.

3.6. Optimization of response time by statistical analysis

Sulfide concentration (X_1) and the pH of the medium (X_2) were deemed as influencer factors of this test and their impact on the response time of the biosensor was assessed. To identify the relation between X_1 and X_2 and their optimum levels, central composite design (CCD) and Response Surface Method were used. To do so, 13 experimental runs were required as per the three-level two-factor fractional factorial CCD.

The coded and non-coded variables are presented in Table 2, whereas the experimental design is shown in Table 3.

TABLE 2 *Coded and non-coded values for the optimization of response time of sulfide detection*

Independent variables	−1	0	1
Sulfide concentration	1 μmol	3 μmol	5 μmol
pH	6.4	7.4	8.4

The statistical design results regarding response time can also be found in Table 3. In order to investigate the relationship between responses and variables, the quadratic polynomial model was derived based on the experimental results of CCD. The modeling results are presented in Table 3. Based on Table 3, in which the P values are depicted, the linear and square effects of X_1 and linear effect of X_2 were found to be remarkable ($P < 0.1$). The model that is proposed as a result of regression coefficients for the response time is expressed as:

$$Y = 49.14 + 14.17X_1 + 4.17X_2 - 2.5X_1X_2 - 11.98X_1^2 + 38.02X_2^2$$

where Y is the response time of the biosensor (Sec), X_1 is the pH, and X_2 is the sulfide concentration. Positive signs of the coefficient in the equation correspond to synergistic effects, whereas negative signs refer to antagonistic effects. The Model F-value of 9.82 suggests that the model is remarkable.

The optimum values of sulfide concentration and pH were 1.26 μM and 6.87, respectively. By substituting these values

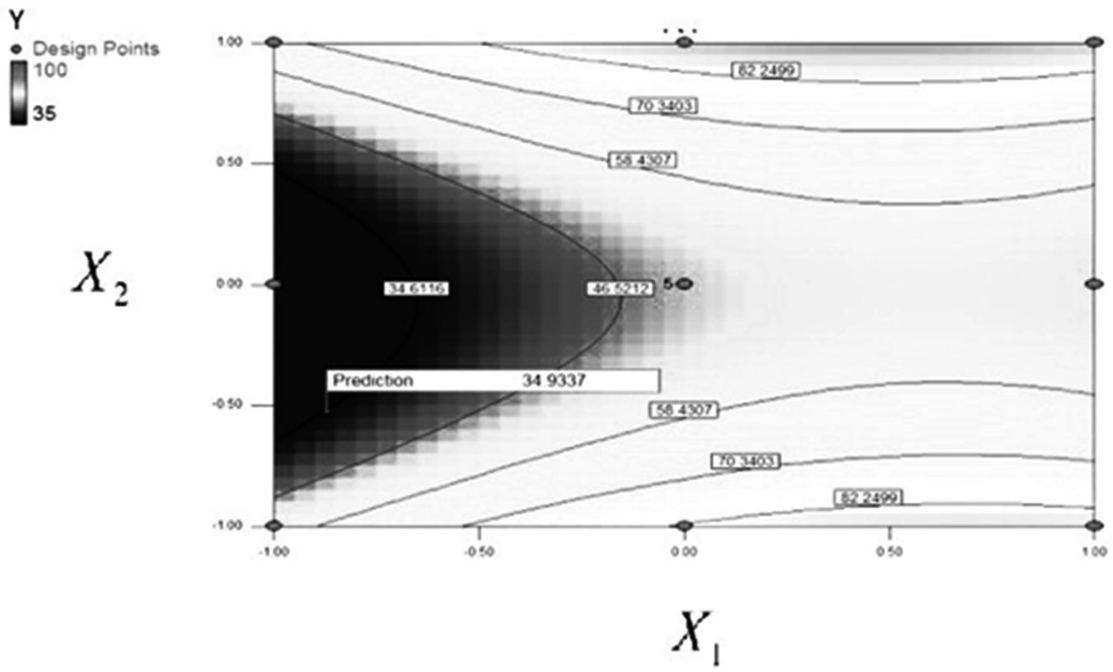

FIG. 7 *Effect of pH and sulfide concentration on biosensor response time.*

TABLE 3 *CCD results for sulfide detection*

Concentration of sulfide	*pH*	*Response time (Sec)*
−1	−1	45
1	−1	80
−1	1	65
1	1	90
−1	0	35
1	0	60
0	−1	100
0	1	95
0	0	45
0	0	40
0	0	45
0	0	40
0	0	45

into the model equation, a detection time of 34.9337 Sec is obtained.

Figure 7 shows the effect of sulfide concentration and pH on the response time of the biosensor. As can be seen, the optimum point (resulting in the minimum detection time) is near the negative coded values of both X_1 and X_2. However, as these values increase to the coded value of 1, which is equivalent to 5 μM for sulfide concentration and pH = 8.4, detection time increases as well.

3.7. Selectivity

To investigate the possible interference in sulfide detection, the effect of the presence of SO_4^{2+} and Fe^{3+} ions in sulfide detection was studied. The results showed that the interference effect of both ions was less than 15%, which confirms sulfide selectivity of this biosensor. Xiong et al. [48] developed an online method for SO_3 detection which selectivity is 73%.

4. Conclusions

In this paper, the applicability of the microfluidic graphene oxide-based biosensor platform for amperometric detection of sulfide was investigated. For this purpose, a biosensor including albumin protein (biological recognition element) and equipped with an amperometry exchanger was designed. The biosensor and biological materials were combined with a microfluidic system, which further reduced reaction time and amount of reagent.

To enhance the surface of electrodes graphene oxide was applied. It also served as a nanosubstrate for loading albumin protein. Hummer's method was used for the synthesis of graphene oxide. Characterization was performed by TEM and FTIR analyses and the high quality of synthesized graphene oxide was observed. Next, by conjugating the protein with graphene oxide, a nanohybrid of graphene oxide–albumin protein was formed. Protein loading on graphene oxide was confirmed by FTIR and potentiostat device results. In the range of 0.5–5 μM, the detection limit was obtained to be 0.5 μM. The effects of pH on the nanosystem were studied in detail, and the optimized pH was evaluated as 7.4. The combination of the microfluidic system caused a remarkable reduction in the response time of the designed biosensor (50 Sec), compare to glassy carbon case (175 S). These results confirm the microfluidic graphene oxide-based biosensor as a fast-response and sensitive device for sulfide detection. The designed biosensor is also portable, which is a result of applying the microfluidic device. The results prove the undeniable role of combining microfluidics and nanotechnology with biomaterials, which can influence the development of new biochips for contaminated and medical detections.

5. References

[1] Colon, M., Todolí, J. L., Hidalgo, M., and Iglesias, M. (2008) Anal. Chim. Acta 609(2), 160–168.
[2] Ebrahimi, E., Yazdian, F., Amoabediny, G., Shariati, M. R., Janfada, B., and Saber, M. (2014) Process Biochem. 49(9), 1393–1401.
[3] Liu, Z., Ma, H., Sun, H., Gao, R., Liu, H., Wang, X., Xu P, and Xun L. (2017) Biosens. Bioelectron. 98, 29–35.
[4] Guenther, E. A., Johnson, K. S., and Coale, K. H. (2001) Anal. Chem. 73(14), 3481–3487.
[5] Greenwood, N. N., Earnshaw, A., (eds.), (1997) Chemistry of the Elements (2nd ed.). pp. 645–746, Butterworth-Heinemann, Oxford.
[6] Atkinson, L. P., and Natoli, J. G. (1974) Reaction 46(5), 346–348.
[7] Puacz, W., Szahun, W., and Linke, K. (1995) Analyst 120(March), 939–941.
[8] Canterford, D. R. (1975) Anal. Chem. 47(1), 88–92.
[9] Koh, T. (1990) Anal. Sci. 6(1), 3–14.
[10] Howard, A. G., and Yeh, C. Y. (1998) Anal. Chem. 70(22), 4868–4872.
[11] Hassan, S. S. M., Marzouk, S. A. M., and Sayour, H. E. M. (2002) Anal. Chim. Acta 466(1), 47–55.
[12] Lawrence, N. S., Jiang, L., Jones, T. G. J., and Compton, R. G. (2003) Anal. Chem. 75(10), 2499–2503.
[13] Yang, Y., Yang, M., Wang, H., Jiang, J., Shen, G., and Yu, R. (2004) Sens. Actuators B 102(1), 162–168.
[14] Zhong, H., Yuan, R., Chai, Y., Li, W., Zhang, Y., and Wang, C. (2011) Bioprocess Biosyst. Eng. 34(8), 923–930.
[15] Rawal, R., and Pundir, C. S. (2012) Int. J. Biol. Macromol. 51(4), 449–455.
[16] Antonietta Baldo, M., Daniele, S., Bragato, C., and Mazzocchin, G. A. (2002) Anal. Chim. Acta 464(2), 217–227.
[17] Kia, M., Islamnezhad, A., Shariati, S., and Biparva, P. (2011) Korean J. Chem. Eng. 28(10), 2064–2068.
[18] Mishra, S. K., Rani, S., and Gupta, B. D. (2014) Sens. Actuators B 195, 215–222.
[19] Omidi, M., Amoabediny, G., Yazdian, F., and Habibi-Rezaei, M. (2015) EPL. 109(1).
[20] El Ichi, S., Abdelghani, A., Hadji, I., Helali, S., Limam, F., and Marzouki, M. N. (2008) Biotechnol. Appl. Biochem. 51(Pt 1), 33–41.
[21] Gupta, S., Murthy, C. N., and Prabha, C. R. (2018) Int. J. Biol. Macromol. 108, 687–703.

[22] Savizi, I. S. P., Kariminia, H. R., Ghadiri, M., and Roosta-Azad, R. (2012) Biosens. Bioelectron. 35(1), 297–301.
[23] Alhadrami, H. A. (2018) Biotechnol. Appl. Biochem. 65(3), 497–508.
[24] Ejeian, F., Etedali, P., Mansouri-Tehrani, H.-A., Soozanipour, A., Low, Z.-X., Asadnia, M., Taheri-Kafrani, A., and Razmjou, A. Biosens. Bioelectron. (2018) 118, 66–79.
[25] Liu, L., Chen, Z., Yang, S., Jin, X., and Lin, X. (2008) Sens. Actuators B 129(1), 218–224.
[26] Periasamy, A. P., Ting, S. W., and Chen, S. M. (2011) Int. J. Electrochem. Sci. 6(7), 2688–2709.
[27] Shan, D., Li, Q. B., Ding, S. N., Xu, J. Q., Cosnier, S., and Xue, H. G. (2010) Biosens. Bioelectron. 26(2), 536–541.
[28] Albery, W. J., Cass, A. E. G., Mangold, B. P., and Shu, Z. X. (1990) Biosens. Bioelectron. 5(5), 397–413.
[29] Poor, N. Z. M., Baniasadi, L., Omidi, M., Amoabediny, G., Yazdian, F., Attar, H., Heydarzadeh, A., Zarami, A. S., and Sheikhha, M. H. (2014) Enzyme Microb. Technol. 63, 7–12.
[30] Janfada, B., Yazdian, F., Amoabediny, G., and Rahaie, M. (2015) Biotechnol. Appl. Biochem. 62(3), 349–356.
[31] Xu, T., Scafa, N., Xu, L.-P., Zhou, S., Abdullah Al-Ghanem, K., Mahboob, S., Fugetsu, B., and Zhang, X. (2016) Analyst 141(4), 1185–1195.
[32] Darwish, N. T., Sekaran, S. D., and Khor, S. M. (2018) Sens. Actuators B 255, 3316–3331.
[33] Wu, J., Dong, M., Santos, S., Rigatto, C., Liu, Y., and Lin, F. (2017) Sensors (Basel, Switzerland). 17(12).
[34] Juang, Y. J., and Chang, J. S. (2016) Biotechnol. J. 11(3), 327–335.
[35] Pol, R., Céspedes, F., Gabriel, D., and Baeza, M. (2017) Trends Anal. Chem. 95, 62–68.
[36] Pan, D., Wang, S., Zhao, B., Wu, M., Zhang, H., Wang, Y., and Zheng, J. (2009) Chem. Mater. 21(14), 3136–3142.
[37] Hermanson, G. T. (2013). Bioconjugate Techniques (3rd ed.). pp. 989–1016, Academic Press, Boston.
[38] Cruys-Bagger, N., Ren, G., Tatsumi, H., Baumann, M. J., Spodsberg, N., Andersen, H. D., Gorton, L., Borch, K., and Westh, P. (2012) Biotechnol. Bioeng. 109(12), 3199–3204.
[39] Akbari Jonoush, Z., Yazdian, F., Mansori, R., and Omidi, M. (2016) Biosci. Biotechnol. Res. Asia 13(4), 2273–2279.
[40] Rana, V. K., Choi, M. C., Kong, J. Y., Kim, G. Y., Kim, M. J., Kim, S. H., Mishra, S., Singh, R. P., and Ha, C. S. (2011) Macromol. Mater. Eng. 296(2), 131–140.
[41] Mirzaei, M., Amoabediny, G., Yazdian, F., Sheikhpour, M., Ebrahimi, E., and Zadeh, B. E. H. (2014) Process Biochem. 49(3), 380–385.
[42] Salamanca-Neto, C. A. R., Scremin, J., Fatibello-Filho, O., Clausen, D. N., and Sartori, E. R. (2018) Analyst 143(15).
[43] Manikkath, J., Manikkath, A., Shavi, G. V., Bhat, K., and Mutalik, S. (2017) J. Drug Deliv. Sci. Technol. 41, 334–343.
[44] Ghadiri, M., Kariminia, H.-R., and Roosta Azad, R. (2013) Ecotoxicol. Environ. Saf. 91, 117–121.
[45] Li, H., Fan, J., Long, S., Du, J., Wang, J., and Peng, X. (2018) Sens. Actuators B 273, 899–905.
[46] Kanik, F. E., Kolb, M., Timur, S., Bahadir, M., and Toppare, L. (2013) Int. J. Biol. Macromol. 59, 111–118.
[47] Wen, T., Yu, J., Jin, E., Liu, T., Hou, X., and Sun, Q. (2019) Sens. Actuators B 279, 177–182.
[48] Xiong, J., Li, Y., Wang, J., Yang, Y., and Zhu, T. (2018) J. Environ. Sci. 72, 25–32.
[49] Vosoughi, A., Yazdian, F., Amoabediny, G., and Hakim, M. (2015) Biosens. Bioelectron. 70, 106–114.
[50] Li, Y., Zhang, X., Zhang, L., Jiang, K., Cui, Y., Yang, Y., and Qian, G. (2017) J. Solid State Chem. 255, 97–101.